Fractional occurrence of defects in membranes and mechanically driven interleaflet phospholipid transport

Robert M. Raphael,[1] Richard E. Waugh,[2,*] Saša Svetina,[3] and Boštjan Žekš[3]
[1]*Department of Biomedical Engineering, Center for Computational Medicine and Biology, Traylor Building, Room 613, Johns Hopkins University School of Medicine, 720 Rutland Avenue, Baltimore, Maryland 21205-2196*
[2]*Department of Biomedical Engineering, University of Rochester School of Medicine and Dentistry, 601 Elmwood Avenue, Box 639, Rochester, New York 14642*
[3]*Institute of Biophysics, Faculty of Medicine, University of Ljubljana, and J. Stefan Institute, 1000 Ljubljana, Slovenia*
(Received 20 October 2000; revised manuscript received 29 June 2001; published 25 October 2001)

The picture of biological membranes as uniform, homogeneous bileaflet structures has been revised in recent times due to the growing recognition that these structures can undergo significant fluctuations both in local curvature and in thickness. In particular, evidence has been obtained that a temporary, localized disordering of the lipid bilayer structure (defects) may serve as a principal pathway for movement of lipid molecules from one leaflet of the membrane to the other. How frequently these defects occur and how long they remain open are important unresolved questions. In this report, we calculate the rate of molecular transport through a transient defect in the membrane and compare this result to measurements of the net transbilayer flux of lipid molecules measured in an experiment in which the lipid flux is driven by differences between the mechanical stress in the two leaflets of the membrane bilayer. Based on this comparison, we estimate the frequency of defect occurrence in the membrane. The occurrence of defects is rare: the probability of finding a defect in 1.0 μm^2 of a lecithin membrane is estimated to be $\sim 6.0\times 10^{-6}$. Based on this fractional occurrence of defects, the free energy of defect formation is estimated to be $\sim 1.0\times 10^{-19}$ J. The calculations provide support for a model in which interleaflet transport in membranes is accelerated by mechanically driven lipid flow.

DOI: 10.1103/PhysRevE.64.051913 PACS number(s): 87.14.Cc, 87.15.He, 87.16.Dg

I. INTRODUCTION

The phospholipid bilayer is the fundamental structural unit of all cellular membranes. Cell membranes contain many different types of lipids, and these lipids are found at different concentrations in the two leaflets of the bilayer. This asymmetrical distribution of lipids is important for the health of the cell. The asymmetry is generated and maintained by proteins that consume metabolic energy and selectively transport lipid molecules from one leaflet to the other [1]. Loss of membrane asymmetry has been implicated in a number of pathologies, including various forms of hemolytic anemia [2], and it is thought to be important in various processes including cell-cell and cell-substrate interactions and cell signaling. For example, imbalances in lipid composition enhance the formation of small vesicles budding from the plasma membrane (endocytosis) [3]. Indeed, it can be argued that membrane asymmetry is intricately linked to cell viability, as the translocation of phosphatidylserine from the inner to outer leaflet is a signal associated with programed cell death, or apoptosis [4,5].

A complete understanding of membrane asymmetry must include not only a description of the specific proteins involved, but also a description of the passive, nonspecific movement of lipid molecules. The hydrophobic interior of cell membranes provides a natural barrier to the movement of lipid molecules from one leaflet to the other because the reorientation of the polar lipid headgroup away from water at the membrane interface and into the hydrocarbon region is energetically unfavorable. Nevertheless, a small but finite rate of lipid transport is observed to occur between membrane leaflets, as lipid molecules diffuse passively across the membrane and tend to reestablish equivalent concentrations on both sides of the membrane. This diffusional transport of lipid molecules between opposing leaflets of bilayer membranes (lipid ''flip-flop'') has been measured by inserting probe molecules (fluorescent or spin-label) into one leaflet of the membrane and measuring their appearance on the other side of the membrane. Such measurements indicate that this diffusional transport is extremely slow, with characteristic times for phosphatidylcholine of many hours or even days [6,7], leading to the prevailing view that passive ''flip-flop'' in pure bilayer membranes is a rare and improbable event.

The nonspecific movement of lipids between leaflets is expected to depend on the physical state and forces applied to the membrane. Recent measurements have indicated that in membranes to which mechanical forces are applied, the transport of lipid molecules between leaflets in a pure bilayer occurs $\sim$100 times faster than expected based on previous measurements employing diffusion of lipid probes [8–10]. In the present report, a model is developed that reconciles the measurements obtained in mechanically strained vesicles with the earlier measurements of passive flip-flop. The model gives new insights into mechanisms and rates of transbilayer lipid flux in membranes subjected to mechanical deformation. Recent theoretical simulations of membrane asymmetry indicate that mechanical effects on lipid translocation rates must be included to correctly predict the asymmetric lipid distribution [11,12].

*Corresponding author. Fax: (716) 273-4746. Email address: waugh@seas.rochester.edu

A number of investigators have argued that the passive movement of lipid molecules between leaflets (''flip-flop'') occurs at membrane defects [13,14]. Membrane defects, often identified as pores, are areas of the membrane where the hydrophobic barrier properties of the membrane temporarily relax. Wimley and Thompson [14] have presented thermodynamic arguments suggesting that flip-flop occurs via defects even in pure fluid bilayers at temperatures far above the gel-liquid crystal phase transition temperature. Here we develop a model for transport via defects based on the assumption that once a defect forms, there is negligible resistance at the defect site for molecules to move from one leaflet of the bilayer to the other. The transbilayer flux of molecules, therefore, depends on the probability that a defect will form, and the rate at which molecules move laterally along the surface to the defect site. In this work, we present an analysis of the transport of lipids to defect sites on both planar and spherical surfaces. This analysis reveals that differences between the rate of diffusion-driven vs mechanically driven transmembrane lipid transport can be reconciled if the transbilayer movement of lipid molecules occurs at localized sites of facile transport (defects) in the membrane. The predictions of the analysis are compared to mechanical measurements reflecting interleaflet lipid transport. From this, we estimate the frequency of occurrence of defects in the membrane and the free energy required for defect formation.

II. MOLECULAR FLUX IN MECHANICALLY STRAINED MEMBRANES

We treat the problem of the transport of lipid molecules laterally along a bilayer membrane surface to a localized site of facile transport between the leaflets. In the following, we consider the driving force for lipid transport to be a difference in mechanical stress supported by the two leaflets of the bilayer. The origin of the stress differences does not bear directly on the analysis, but such differences might result from membrane deformation or asymmetric changes in membrane composition. We express the stress difference in terms of the difference in the area strains on the two leaflets. The stress is directly proportional to the strain because the area dilation of phospholipid membranes is small. The area strain α is defined separately for each leaflet as the change in the local leaflet area relative to its stress-free area ($\alpha = \Delta A/A_0$). For a bilayer membrane, the difference between the strain on the outer leaflet α_+ and the strain on the inner leaflet α_- is $\alpha_\pm = \alpha_+ - \alpha_-$. In terms of area per molecule over the surface of the membrane, $\alpha_\pm$ may be considered a differential dilation field.

We characterize a defect as a connection between the two leaflets in a localized circular region of radius r_d allowing the movement of molecules from the compressed to the expanded leaflet. As molecules move from one leaflet to the other, the stress difference, and consequently $\alpha_\pm$, is reduced in the vicinity of the defect (Fig. 1). If the resistance to transport through the defect itself is negligible, the transport of molecules to and from the defect site is limited by the lateral transport of molecules along the surface in the vicinity of the defect, toward the defect site on the compressed leaflet and away from the defect site on the expanded leaflet. This movement alters the gradient in $\alpha_\pm$ in the vicinity of the defect, which further drives differential flow to the defect. To analyze this problem, we employ a model developed by Evans and Yeung [15,16] for the dynamics of lipid surface flow driven by gradients in interleaflet stress differences. In this model, dissipation of differential density gradients occurs by flow of the expanded leaflet relative to the compressed leaflet: differential stress gives rise to differential velocity between the membrane leaflets. Designating the velocity of the outer leaflet as ν_+ and that of the inner leaflet as ν_-, the relative velocity between the leaflets is $\nu_\pm = \nu_+ - \nu_-$. The differential velocity $\nu_\pm$ is related to the differential dilation $\alpha_\pm$ by an equation derived from force balance [17]:

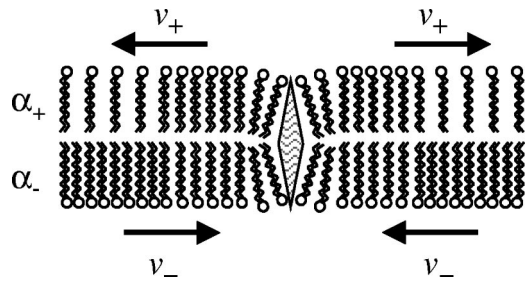

FIG. 1. Schematic of mechanically driven transport through a defect region. The defect is graphically represented by the diamond in the figure. When a defect forms, material from the compressed inner leaflet moves to the defect site and is transported to the expanded outer leaflet. Due to rapid transport at the defect site, the differential density is rapidly equilibrated in the vicinity of the defect (see Fig. 3).

$$\vec{\nu}_\pm = D_m \ \text{grad}\ \alpha_\pm . \tag{1}$$

Hence the magnitude of the relative motion between the membrane leaflets will be proportional to the magnitude of the local spatial gradient of $\alpha_\pm$, scaled by D_m, the coefficient of mechanical diffusivity. Physically, D_m characterizes the ratio of the elastic driving force to the viscous resistance to relative motion. In keeping with the development published by Evans and Yeung [15], D_m is proportional to the ratio of the elastic area compressibility modulus of the membrane K to the coefficient of interleaflet drag b: $D_m = K/4b$. The physical origin of b is that relative leaflet motion will be opposed by drag at the interface between the hydrocarbon chains. This shear stress exerted at the center of the bilayer by one leaflet on the other, σ_c, is assumed to be proportional to the differential velocity of the two leaflets relative to each other: $\sigma_c = b\nu_\pm$. The interlayer drag coefficient (b) has been measured in tether pulling experiments [8,15] and has a value of $(1-4)\times 10^8$ (N·s)/m^3. For a typical phosphatidylcholine bilayer with $K = 200$ mN/m, D_m is predicted to be $\sim 5\times 10^{-6}$ cm^2/s.

It is convenient to describe the transport of molecules along the surface in terms of a lateral flux $j_\pm$ defined as

$$\vec{j}_\pm = \frac{1}{\tilde{A}}\vec{\nu}_\pm , \tag{2}$$

where $\tilde{A}$ is the stress-free area per molecule. The lateral flux occurs as a result of gradients in the differential density $\alpha_{\pm}$, and, in general, is a function of position and time. A governing equation for the distribution of the differential density field can be derived by taking the divergence of both sides of Eq. (1), employing Eq. (2) and invoking surface continuity. Neglecting small terms leads to a governing equation for the time evolution of the differential density [15]:

$$\frac{\partial \alpha_{\pm}}{\partial t} = D_m \nabla^2 \alpha_{\pm}. \tag{3}$$

This equation can be solved for different geometries by choosing the appropriate Laplace operator. Note that Eq. (3) is identical in form to the diffusion equation. The differential density is analogous to a local surface concentration and D_m is analogous to D_l, the lateral diffusion coefficient. As such, the problem is formally the same as a transport problem driven by gradients in surface concentration, and so comparisons between mechanically driven and diffusion-driven transport can readily be made.

When a defect forms, the differential dilation field drives the lateral flux of molecules along the surface to the site where they are transported across the membrane. The number of molecules moving from one leaflet to the other per unit time through the defect is simply the product of the flux and the perimeter length of the defect. Noting that one molecule moving from one leaflet to the other counts twice in reducing the difference in the number of molecules between leaflets, the flux through a defect can be written as

$$\frac{dn}{dt} = \frac{1}{2} \int (\vec{j}_{\pm} \cdot \vec{n}) dl, \tag{4}$$

where $\vec{n}$ is the normal vector to the edge of the defect within the plane of the membrane and dl is the perimeter length (which integrates to $2\pi r_d$ for the case of a circular defect). The instantaneous flux dn/dt is considered positive for molecules moving from the inner $(-)$ leaflet to the outer $(+)$ leaflet. The total number of molecules that move across the membrane during the lifetime of the defect is the integral of the instantaneous flux in Eq. (4) over the defect lifetime:

$$\Delta n = \int_0^{t_{\mathrm{lif}}} \frac{dn}{dt} dt. \tag{5}$$

Equations (1)–(5) constitute the theoretical framework for our analysis of mechanically-driven interleaflet transport.

III. SPATIAL DISTRIBUTION OF DIFFERENTIAL DENSITY AND NET MOLECULAR FLUX

To calculate the flux to a defect, the differential density field must be known over the surface of the vesicle and then evaluated at the location of the defect. We approach this problem in two different ways. First, we formulate the problem realistically as a hole that forms on a spherical surface. The resulting solution for the flux is an infinite series of Legendre polynomials that must be evaluated numerically. In a complementary approach, we consider the defect as a hole in a planar region. The solution in the planar region has the advantage that a closed form analytic solution is obtained for the molecular flux and expressed as an integral of Bessel functions. A comparison of the two solutions reveals the defect lifetimes for which precise geometric considerations affect the solution to the problem.

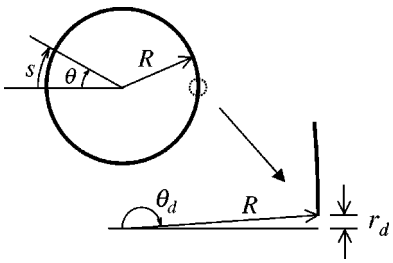

FIG. 2. Geometry of the defect problem. The angle θ is taken from the side of the vesicle opposite the defect. The coordinate distance along a surface meridian is s. The vesicle is assumed to be spherical with radius R. The defect is located at an angle $\theta_d \cong \pi$, and $\sin \theta_d \approx r_d/R$ (see inset). This relation is used in calculating the indices of the nonintegral Legendre polynomials.

A. Formulation and solution on the spherical vesicle

Consider a spherical phospholipid vesicle of radius R with a uniform difference in the area strain between the adjacent leaflets. At time $t=0$ a circular defect of radius r_d forms on the surface of the membrane at an angle $\theta_d \approx \pi$ from the origin of the coordinate system (Fig. 2). At this location, material moves through the defect from the compressed side of the membrane to the expanded side in order to equilibrate $\alpha_{\pm}$. In the curvilinear coordinate system shown in Fig. 2, the governing equation for the evolution of $\alpha_{\pm}$ takes the form

$$\frac{\partial \alpha_{\pm}}{\partial t} = \frac{D_m}{R^2} \left(\frac{\partial^2 \alpha_{\pm}}{\partial \theta^2} + \cot \theta \frac{\partial \alpha_{\pm}}{\partial \theta} \right). \tag{6}$$

The initial and boundary conditions for the problem are as follows:

$$\alpha_{\pm}(\theta, 0) = \alpha_0 \quad \text{for any} \quad \theta < \theta_d, \tag{7a}$$

$$\alpha_{\pm}(\theta_d, t) = 0, \tag{7b}$$

where α_0 is the initial, uniform value of the differential density on the vesicle prior to the formation of the defect. The solution to this problem is obtained by the standard technique of separation of variables [18,19]:

$$\alpha_{\pm}(\theta, t) = \alpha_0 \sum_{s=0}^{\infty} A_s P_{\nu_s}(\cos \theta) e^{-k_s t}$$

where

$$k_s = \frac{\nu_s(\nu_s + 1) D_m}{R^2} \tag{8}$$

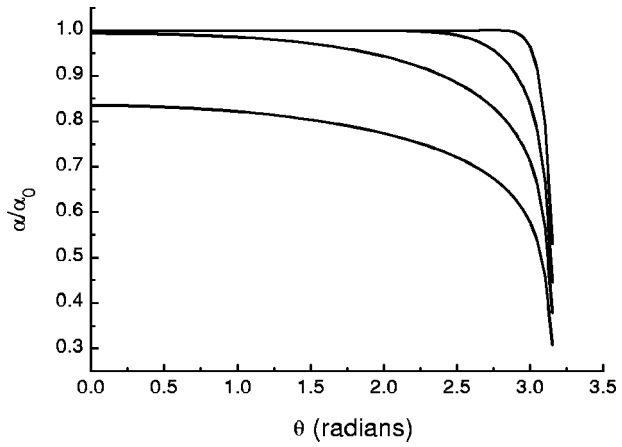

FIG. 3. Plot of $\alpha_{\pm}$ at successive times after defect formation. At time $t=0$, a defect forms on the surface of the vesicle at the location $\theta=\pi$. The normalized value of $\alpha_{\pm}(\alpha_{\pm}/\alpha_0)$ is plotted versus the location on the surface of the vesicle. The successive curves (from top to bottom) are the distribution of $\alpha_{\pm}$ on the surface at $t=0.001$, $t=0.01$, $t=0.1$, and $t=0.5$ s after a defect forms. For short defect lifetimes, significant changes in $\alpha_{\pm}$ only occur in the region near the defect. Propagation of the changes in $\alpha_{\pm}$ far from the defect site requires times on the order of 0.1 s or greater. ($r_d=2.7$ nm.)

and where ν_s are the nonintegral values of the Legendre function, which satisfy the boundary condition. The values ν_s depend on the cosine of the angle at the location where the Legendre function must vanish and can be obtained from previously derived formulas [20]:

$$\nu_s = s + \frac{1}{\ln\left(\frac{2}{1+\mu_0}\right) - 2\sum_s \frac{1}{s}} \quad \text{where} \quad \mu_0 = \cos(\theta_d). \tag{9}$$

The expansion coefficients A_s are calculated from the orthogonality property and can be expressed as [20]

$$A_s = \frac{I_s}{H_s}, \tag{10a}$$

$$I_s = \frac{\sin(\nu_s\pi)}{\pi}\left[\frac{2}{\nu_s(\nu_s+1)} + (1+\mu_0)\right], \tag{10b}$$

$$H_s = \frac{2}{2\nu_s+1}\left[1 - \frac{2\sin^2(\nu_s\pi)}{\pi^2}\psi'(\nu_s+1) - (2\nu_s+1)\frac{\sin^2(\nu_s\pi)}{\pi^2}(1+\mu_0)\right], \tag{10c}$$

where $\psi'(\nu_s+1)$ is the polygamma function.

The spatial and temporal aspects of the solution in Eq. (8) are illustrated graphically in Fig. 3. The value of $\alpha_{\pm}$, scaled by α_0, is plotted versus the location on the surface from the defect. As shown, the differential density equilibrates rapidly in the region of the defect and then begins to equilibrate over the entire surface.

To calculate the flux, the solution for $\alpha_{\pm}$ [Eq. (8)] is inserted into Eqs. (1), (2), and (4) and expanded by the chain rule to obtain

$$\frac{dn}{dt} = \frac{\pi r_d}{\tilde{A}}\frac{D_m\alpha_0}{R}\sin\theta_d\sum_{s=0}^{\infty} A_s\frac{\partial P_{\nu_s}(\cos\theta_d)}{\partial(\cos\theta_d)}e^{-k_s t}. \tag{11}$$

The net movement of molecules through a defect is found by applying Eq. (5) and integrating the instantaneous molecular movement over the defect lifetime (t_{lif}):

$$\Delta n = \frac{\pi r_d^2\alpha_0}{\tilde{A}}\sum_{s=0}^{\infty}\frac{A_s P'_{\nu_s}}{\nu_s(\nu_s+1)}(1-e^{-k_s t_{\text{lif}}}), \tag{12}$$

where we have taken $\sin\theta_d = r_d/R$ and have written the partial derivative of the nonintegral Legendre functions with respect to $\cos\theta$ as P'_{ν_s}. These derivatives can be calculated via the formulas previously presented [20]:

$$P'_{\nu_s} = \frac{\nu_s(\nu_s+1)}{1-\mu_0^2}\frac{\sin(\nu_s\pi)}{\pi}\left[\frac{2}{\nu_s(\nu_s+1)} + (1+\mu_0)\right]. \tag{13}$$

The term Δn will have units of number of molecules, and the average rate of molecular transport through a defect will be Δn divided by the lifetime of the defect.

B. Formulation and solution in the planar region

The solution in the spherical region, while having the advantage of being an exact solution, is an infinite series that converges very slowly. In order to validate this solution, we therefore formulated the problem in a planar region in a polar coordinate system. This gives us an analytic solution that can be integrated to estimate the molecular flux as a function of the lifetime of the defects (t_{lif}). This problem has been treated previously [21]. The governing equation for the problem is

$$\frac{\partial\alpha_{\pm}}{\partial t} = \frac{1}{r}\frac{\partial}{\partial r}(rD_m)\frac{\partial\alpha_{\pm}}{\partial r}. \tag{14}$$

The boundary conditions of this problem are that the initial value of $\alpha_{\pm}$ (designated α_0) is constant in the region of interest but the value of $\alpha_{\pm}$ at the defect itself is zero:

$$\alpha_{\pm}(r,0) = \alpha_0, \quad r > r_d,$$
$$\alpha_{\pm}(r_d,t) = 0. \tag{15}$$

The solution is expressed as an integral of Bessel functions:

$$\alpha_{\pm}(r,t) = \alpha_0 - \frac{2\alpha_0}{\pi}\int_0^{\infty}\exp(-D_m u^2 t_{\text{lif}}/r_d^2) \times \frac{J_1(ru/r_d)Y_0(u) - Y_1(ru/r_d)J_0(u)}{J_0^2(u)+Y_0^2(u)}\frac{du}{u}, \tag{16}$$

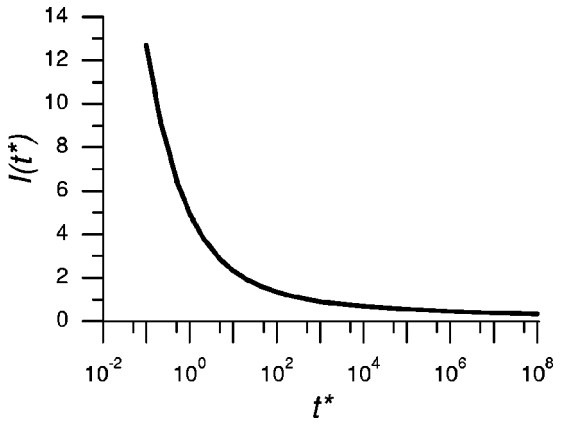

FIG. 4. Solution for a planar geometry. The solution is expressed in terms of the dimensionless parameter t^*. The solution $I(t^*)$ has a steep dependence on the pore lifetime for characteristic times less than r_d^2/D_m because on this time scale the spatial distribution of $\alpha_\pm$ changes rapidly. The pore lifetimes we consider (1.0 μs to 0.1 s) correspond to the region where $0.63<\ln t^*<5.6$.

where J_0 and Y_0 are Bessel functions of the first and second kind, respectively, and J_1 and Y_1 are the negative of their derivatives. The solution for the concentration as a function of time can be converted to a flux of molecules by applying Eqs. (1), (2), and (4),

$$\frac{dn}{dt}=\frac{4\alpha_0 D_m}{\pi\tilde{A}}\int_0^\infty \exp(-D_m u^2 t_{\rm lif}/r_d^2)\,\frac{1}{J_0^2(u)+Y_0^2(u)}\,\frac{du}{u}. \tag{17}$$

The number of molecules that pass through the defect is then obtained by Eq. (5) and expressed as

$$\Delta n=\alpha_0 D_m t_{\rm lif} I(t^*)/\tilde{A} \tag{18}$$

where

$$I(t^*)=\frac{4}{\pi t^*}\int_0^\infty \frac{1-e^{-t^* u^2}}{J_0^2(u)+Y_0^2(u)}\,\frac{du}{u^3} \quad \text{and} \quad t^*=\frac{D_m t_{\rm lif}}{r_d^2}. \tag{19}$$

Note that for a ''typical'' defect with a radius of 2.7 nm and a lifetime of 1.0 μs, $t^*\approx 70$. Figure 4 shows the results of numerical integration of the characteristic function $I(t^*)$ as a function of the defect lifetime.

IV. RESULTS

The numerical values of Δn were calculated by evaluating either Eq. (12) or Eq. (18) for a chosen defect size and lifetime. In the spherical solution, this evaluation required the calculation of the expansion coefficients A_s, the nonintegral values of the Legendre polynomials ν_s and the derivative of the nonintegral Legendre functions. These quantities were evaluated on an Irix System V.4 by using a mathematical computation software (MATHEMATICA, Wolfram Research). The initial value of $\alpha_\pm$ was taken to be 0.007 and D_m was taken to be 5×10^{-6} cm^2/s. The radius of the vesicle was taken to be 8 μm and the radius of the defect was initially taken to be the monolayer separation distance, h (2.7 nm). The infinite series in Eq. (12) converges. However, for short defect lifetimes, this convergence is slow due to the slow falloff of the exponential term. Therefore, it is important to know how many terms must be included in the expansion in Eq. (10) to reach sufficient accuracy. In practice, the series was evaluated until the next term was smaller than 10^{-6} times the current partial sum. Graphical inspection of a plot of the partial sums plotted versus the number of terms also indicated that convergence was reached at this point. The number of terms that needed to be evaluated depended on the defect lifetime and radius. For a 2.7 nm defect open for 100 ms, the series needed to be evaluated to 90 terms. The calculations indicate that 2.8×10^5 molecules move through the defect during the 100 ms that it is open. For $t_{\rm lif}=10$ ms, the series was evaluated to 216 terms and 3.3×10^4 molecules move across the defect. For $t_{\rm lif}=1.0\,\mu$s, the series needed to be evaluated to 1927 terms and approximately 11 molecules move across the defect. Larger defects required more terms in the series to be evaluated, especially at shorter lifetimes. The net flux of molecules for different defect lifetimes are given in Table I. The calculated flux depends on the radius of the defect, as the eigenvalues ν_s depend on the geometry of the region in

TABLE I. Number of molecules transported as a function of defect lifetime and defect radius. The entries Δn (no. of molecules per defect) are calculated from Eq. (12) for the spherical region and from Eq. (18) for the planar region.

Defect lifetime $t_{\rm lif}$ (s)	Defect radius (nm)					
	2.7		5.4		10.8	
	Δn spherical	Δn planar	Δn spherical	Δn planar	Δn spherical	Δn planar
10^{-6}	11.0	10.2	14.7	14.1	18.0	20.9
10^{-5}	71.6	68.1	91.6	85.6	121.4	113.2
10^{-4}	517.6	506.7	621.0	599	722.1	732.6
10^{-3}	4.05×10^3	4.01×10^3	4.65×10^3	4.58×10^3	5.46×10^3	5.34×10^3
10^{-2}	3.32×10^4	3.32×10^4	3.71×10^4	3.71×10^4	4.21×10^4	4.19×10^4
10^{-1}	2.80×10^5	2.84×10^5	3.07×10^5	3.11×10^5	3.40×10^5	3.44×10^5

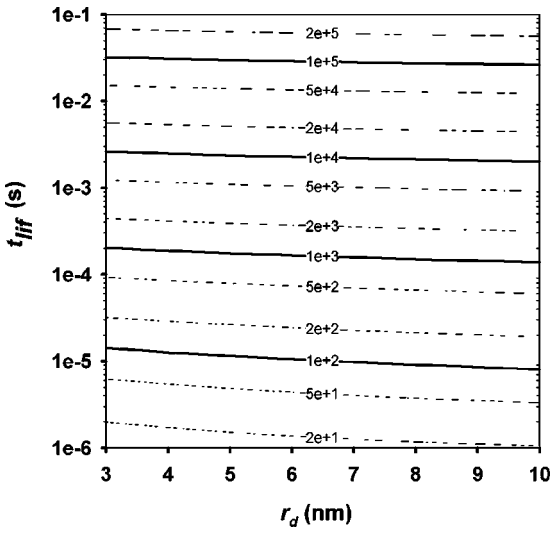

FIG. 5. A contour plot of Δn as a function of defect lifetime and radius. The curves in the figure are labeled to indicate the number of molecules transported through the defect as a function of defect radius and lifetime. Curves are shown for Δn ranging from 20 to 200 000 molecules. For the range of values considered, there is only a weak dependence of Δn on the radius of the defect.

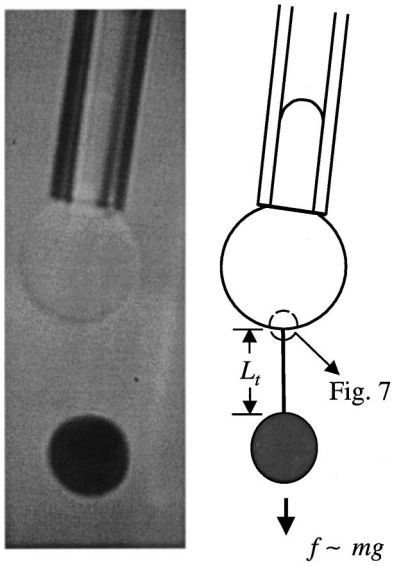

FIG. 6. A videomicrograph (left) and schematic (right) of the mechanical experiment used to measure the rate of mechanically driven interleaflet lipid transport. A phospholipid vesicle aspirated into a micropipette is brought into adhesive contact with a glass bead. When the holding pressure in the pipette is reduced, a thin microtube (tether) is pulled out under the force of gravity. The radius of the tether is on the order of 10–100 nm, too small to be visible with the light microscope. The tether is a source of differential area due to the geometry of the membrane pulled into a cylindrical tube (see Fig. 7). The differential area relaxes over the surface of the vesicle by membrane surface flow limited by interlayer drag and transbilayer movement of molecules occurring at membrane defects.

which the differential density gradient must vanish. Increasing the defect radius from h (2.7 nm) to $2h$ or $4h$ increases the number of molecules that pass through the defect, but this dependence is relatively weak, as illustrated in Fig. 5.

The two approaches for calculating the number of molecules that pass through a defect are in close agreement, providing important validation of the numerical results. For the shortest defect lifetimes, the calculations based on the planar geometry are likely to be more accurate, because of the very slow convergence in this regime of the infinite Legendre series obtained for the spherical solution. The numerical accuracy for the planar solution appears to be relatively insensitive to pore lifetime over the pore lifetimes of interest. This is evident from Fig. 4 in which the value of the characteristic function $I(t^*)$ is shown to be well behaved over the relevant range of pore lifetimes.

V. COMPARISON WITH EXPERIMENTALLY MEASURED TRANSBILAYER FLUXES

The rate at which phospholipid molecules move from one membrane leaflet to the other in response to stress differences between the leaflets has been measured in micromechanical experiments on phospholipid vesicles [8,9]. The experiments involved the formation of thin tubular lipid strands (tethers) approximately 30 nm in radius from the surfaces of giant unilamellar phospholipid vesicles. The vesicles ($\sim$20–30 μm diameter) were aspirated into micropipettes and attached to small glass beads (Fig. 6). Initially the tension in the membrane generated by the aspiration pressure in the micropipette was large enough to hold the bead in close contact with the vesicle, but when the aspiration pressure was reduced, the bead fell away from the vesicle under the force of gravity, forming the tether between the bead and the body of the vesicle. Mechanical equilibrium could be established by adjusting the aspiration pressure such that the membrane tension was sufficient to balance the gravitational force on the bead [22,23].

Formation of a tether from a bilayer membrane results in an expansion of the outer membrane leaflet relative to the inner leaflet because of the difference in the radii of the two leaflets in the tether (Fig. 7). The length of the tether provides a direct measure of the total difference in area between the leaflets over the vesicle: as the tether length increases the differential area increases proportionally. In the absence of lipid transport between leaflets, a change in the membrane tension from a particular equilibrium state should result in a change to a new equilibrium tether length, at which the elastic energy stored in the differential dilation between the leaflets exactly compensates for the change [23]. A dynamic model incorporating dissipation of differential density by interlayer drag also predicted that a new equilibrium should be reached [17]. However, this expected approach to equilibrium was not observed experimentally. Rather, the tether continued to grow beyond the expected equilibrium length at a rate proportional to the stress difference between the leaflets generated by the perturbation [8,9]. The relative expansion/compression of the area per molecule of the two leaflets is proportional to the stress difference between the leaflets, which must have a particular value to satisfy the mechanical equilibrium. Therefore, the continued growth of

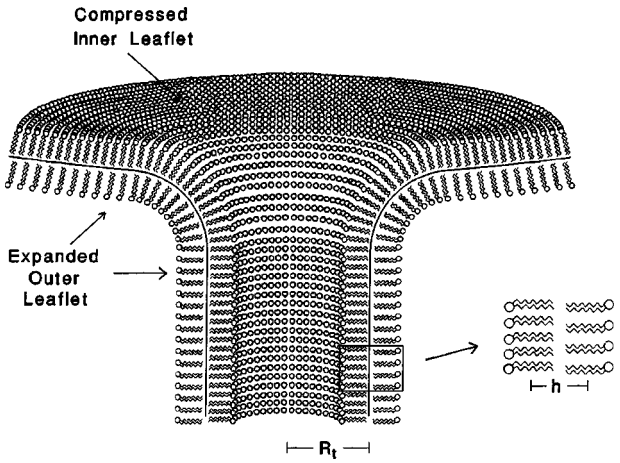

FIG. 7. Illustration of area difference in the tether. Because less material moves into the inner leaflet than into the outer leaflet of the tether, the outer leaflet of the vesicle is slightly expanded and the inner leaflet is slightly compressed. The degree of expansion/compression is exaggerated in the drawing for illustrative purposes. Initially the differential area is concentrated in the vicinity of the tether, but becomes uniform over the surface of the vesicle because leaflets can slide relative to each other. This differential dilation drives the transport of molecules from the compressed inner leaflet to the expanded outer leaflet. Measurement of the tether length provides a sensitive measure of the area difference between the leaflets. For example, a tether with a length of 300 μm formed from a vesicle with a surface area of 1000 μm^2 corresponds to a net increase in the outer leaflet (and an equal decrease in the inner leaflet) of 0.5%.

the tether cannot be attributed to continued expansion and compression of the adjacent leaflets, but rather reflects changes in the relative number of molecules in each leaflet. The rate of tether growth revealed the rate at which molecules move from the compressed inner leaflet to the expanded outer leaflet. This transport is characterized in terms of a phenomenological coefficient c_p, which relates the relaxation rate of the strain differences ($\partial\alpha_\pm/\partial t$) to the magnitude of the strain difference ($\alpha_\pm$). The phenomenological coefficient c_p is related to the net molecular flux across the membrane by [9,19]

$$\Phi_{\text{expt}}=\frac{1}{A_0}\frac{dn}{dt}=\frac{c_p\alpha_\pm}{\tilde{A}}, \tag{20}$$

where A_0 denotes the area of the membrane. The value of c_p obtained in tether formation experiments [8] was $\sim 0.01\ s^{-1}$. For a typical experiment in which $\alpha_\pm=0.007$, the measured flux was $\sim 6.3\times 10^9$ molecules/($cm^2\cdot s$).

VI. PROBABILITY AND FREE ENERGY OF DEFECT FORMATION

The number of molecules that pass through a defect (Δn) as a function of its lifetime were calculated above. The average rate of molecular transport through a defect will be Δn divided by the lifetime of the defect:

$$J_{\text{def}}=\frac{\Delta n}{t_{\text{lif}}}. \tag{21}$$

The surface flux over an entire membrane (Φ_{th}) will be determined by the number of defects that exist in the membrane at a given time. Designating the frequency of occurrence per unit area per unit time for a defect of a particular size and lifetime to be ν, the macroscopically observable flux per unit area of membrane per unit time would be

$$\Phi_{\text{th}}=\Delta n\,\nu, \tag{22}$$

where Φ_{th} has units of $l/(m^2\cdot s)$. The quantity Δn can be regarded as a conductance per defect and depends on the defect lifetime (t_{lif}). If we consider a typical vesicle that has a surface area of 1000 μm^2, our measured experimental flux reported above [6.3×10^9 molecules/($cm^2\cdot s$)] corresponds to 6.3×10^4 molecules moving across the vesicle surface per second. Comparison of this rate to the theoretical calculations of the net molecular transport through a single defect enables us to estimate how frequently defects form in the membrane. For example, using the values in Table I, for a defect with a radius of 2.7 nm and a defect lifetime of 1.0 ms, there would have to be approximately 16 defects forming per second in a vesicle with a surface area of 1000 μm^2. A defect lifetime of 100 μs would require approximately 122 defects to form per second, a lifetime of 10 μs would require 880 defects to form per second, and so on.

Unfortunately, knowledge of the macroscopically measured rate of interleaflet transport does not enable us to specify both the defect lifetime and the frequency of occurrence of defect. However, it does enable us to estimate the probability that a defect will exist at any instant of time. Experimental observation of tethers growing smoothly without apparent stochastic variability indicates that defect lifetimes are short on a time scale of seconds. If we divide both sides of Eq. (22) by J_{def}, which corresponds to taking the ratio of the macroscopic flux obtained from experiment to the calculated mean flux for a single defect, we obtain

$$\frac{\Phi_{\text{expt}}}{J_{\text{def}}}=\nu t_{\text{lif}}=N_d, \tag{23}$$

where N_d is the defect density, or frequency of occurrence per unit area. The numerical results indicate that, on average, there will be 573–2250 defects in a centimeter square of membrane at any given time, depending on the defect lifetime (see Fig. 8). For a defect lifetime of 1 μs, the probability of finding a defect in a 1.0 μm^2 patch of membrane at any given time is about 1 in 175 000.

Knowing the probability of finding a defect in a given area of membrane, and assuming that defect formation follows Boltzmann statistics, we can estimate the free energy cost associated with defect formation. We take the area of a defect to be the area of a disk 2.7 mm in radius ($2.3\times 10^{-5}\ \mu m^2$). At any given instant, we expect to find one such defect in an area of 175 000 μm^2. Thus, the prob-

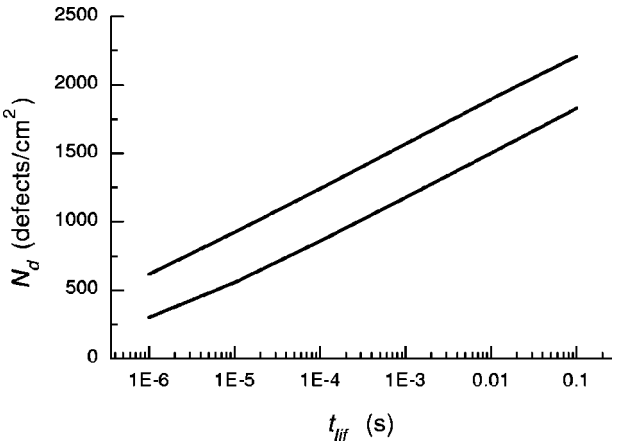

FIG. 8. Density of defects as a function of lifetimes of defects of radius 2.7 nm (top curve) and 10.8 nm (bottom curve). The frequency of defect occurrence per unit area (N_d) calculated from Eq. (23) is that needed to account for the experimentally measured flux assuming all defects have a specific lifetime (corresponding to the value along the horizontal axis).

ability of a small membrane region existing in the defect state rather than the bilayer state is $\sim 1.3\times 10^{-10}$. Boltzmann statistics requires that

$$\frac{P_{\rm def}}{P_{\rm bl}} = \exp(-\Delta G_{\rm def}/k_B T), \tag{24}$$

where $P_{\rm def}$ is the probability that a given collection of molecules will exist as a defect, and $P_{\rm bl}$ is the probability that it will exist in the bilayer state. The energy difference between the two states is

$$\Delta G_{\rm def} \sim 0.9\times 10^{-19}\ \text{J/defect}$$

and is relatively independent of the defect lifetime.

VII. DISCUSSION

We have presented a model in which mechanical stress increases the rate of transbilayer movement of molecules by increasing the rate at which molecules move laterally to a defect site. We have calculated the molecular flux through a single defect and used this in combination with the total molecular flux measured in micromechanical experiments to estimate the probability and free energy of defect formation. Below, we discuss evidence for the occurrence of defects, the relation of our model to equilibrium exchange measurements of lipid flip-flop, and the biological significance of this work.

Defects arise from molecular motions of ensembles of phospholipid molecules. Monte Carlo simulations of the molecular dynamics of lipids predict the existence of ''lateral density fluctuations'' in the membrane [24]. These random alterations in bilayer structure explain a number of phenomena that require a temporary relaxation of the barrier function of the membrane such as permeability changes associated with phase transitions [25,26] and the insertion of nonbilayer lipids in the membrane [27–29]. Defect formation also plays a role in other membrane phenomena such as the passive permeability of the membrane to small molecules and ions [30,31], insertion of catalytic enzymes such as phospholipase A_2 into the bilayer [27,32,33] and flip-flop of molecules from one leaflet to the other [13,14]. The lifetime of these defects is difficult to measure. Dynamic fluorescence measurements in combination with laser temperature jump experiments revealed time constants for collective motions of lipid molecules on the order of microseconds to milliseconds [34,35].

The free energy of defect formation we estimated here compares reasonably with estimates of the free energy associated with pore formation reported by other investigators. Zhelev and Needham [36] measured the membrane tension needed to maintain membrane pores generated by electric fields and mechanical tension. They calculated the energy per unit length of a pore edge to be 1.0×10^{-11} J/m. An independent theoretical analysis of this experiment [37] estimated the line tension to be 2.6×10^{-11} J/m. Shillcock and Boal [38] performed computer simulations of hole formation in membranes and estimated the minimum value of the edge tension required for membrane stability to be 0.9×10^{-11} J/m. If we suppose that the defect is in fact a pore with a radius of 2.7 nm, and use a line tension of 1.0×10^{-11} J/m, we obtain an energy of 1.7×10^{-19} J/defect, which is slightly larger than our estimate based on Boltzmann statistics. Considering the uncertainties and approximations in the various calculations, this agreement seems rather good, although the energy required to form a temporary defect capable of allowing passage of molecules between leaflets may be slightly less than the energy required to form a complete membrane pore. Alternatively, the variations may be related to the size of the defect formed in the different situations.

It is of interest to compare the frequency of defect formation predicted from measurements of mechanically driven lipid transport with that obtained from measurements of interleaflet transport obtained by chemical methods. Wimley and Thompson [14] used chemical probes to measure the rate of lipid ''flip'' in dimyristoylphosphatidylcholine membranes, and argued that this transport occurs through transient defects. The transport of lipid therefore depends on the probability that a defect will exist, and the rate at which probe molecules diffuse to the defect site. The formulism describing the lateral diffusion of lipid probes is identical to the formulism describing mechanically driven transport, except that the characteristic coefficient is the lateral diffusion coefficient $D_l \sim 5.0\times 10^{-8}\ \text{cm}^2/\text{s}$ [39] rather than D_m ($5.0\times 10^{-6}\ \text{cm}^2/\text{s}$) (see Fig. 9). Consequently, significant differences in net transport are expected for concentration-driven vs mechanically driven diffusivity because $D_m \sim 100 D_l$. We can apply the methodology described above to the lateral diffusion case and calculate the net flux of molecules through a defect when the transport is driven by gradients in surface concentration. If there is an initial uniform concentration of probe molecules of 1.0% in one leaflet and zero in the other, then for $t_{\rm lif} = 1.0\ \mu$s, the mean flux per

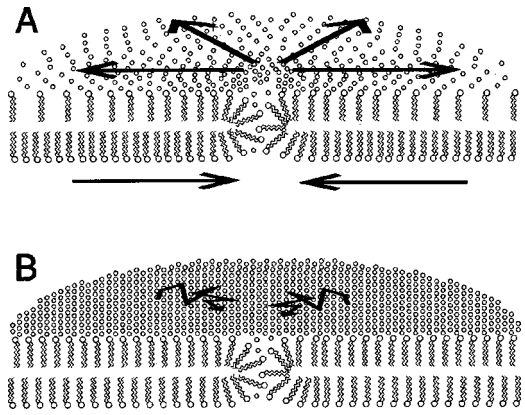

FIG. 9. Mechanical vs molecular diffusion. (a) In mechanically driven lipid transport, the elastic compression of the molecules on the inner leaflet drives the transport of molecules through the defect site onto the expanded outer leaflet. The relative motion between the leaflets is resisted by a frictional interaction at the midplane of the bilayer. (b) In diffusion-driven transport, molecules diffuse randomly on the surface, and the net flux of molecules through the defect is driven by gradients in the concentration of probe molecules.

defect is 2.8×10^5 molecules/s. For comparison, we define an effective diffusive permeability coefficient c_d:

$$\frac{\partial \Delta c}{\partial t} = c_d \Delta c, \tag{25}$$

where Δc is the concentration difference between the two leaflets of the bilayer. Using the rates of interleaflet transport in dimyristoylphosphatidylcholine (DMPC) membranes measured by Wimley and Thompson, we obtain a value for c_d of $1.4\times10^{-4}\,\mathrm{s}^{-1}$ which corresponds to an instantaneous macroscopic flux of molecules across the membrane of 1.4×10^8 molecules/(cm$^2\cdot$s). Comparing this value with the mean flux per defect, we estimate the probability of defect occurrence to be 500 cm^{-2}, which means that the probability of finding a defect in a 1.0 μm^2 patch of membrane at any given time is about one in 200 000. Because DMPC was used in chemical probe experiments and stearoyloleoylphosphatidylcholine in mechanical deformation experiments, the frequency of defect formation may not be exactly the same. DMPC membranes are thinner and might be more susceptible to defect formation. Nevertheless, the close agreement between the calculated probability of defect occurrence in these different experimental approaches supports the general applicability of the model to the mechanism of interleaflet lipid transport.

The enhancement of transbilayer flux caused by differences in mechanical stress between leaflets is distinct from enhancement in flux that might result from increases in the mean stress in the membrane. The latter could result if the number and size of defects depend on the lateral tension in the membrane. Electric fields and osmotic swelling of vesicles produce stresses that facilitate pore formation [36,40]. Although such stress effects (differential and mean) may be additive in some circumstances, the magnitude of the tension in the tether experiment was small compared to the tensions needed to affect pore formation. In fact, the rate of interlayer permeation did not depend on the value of the membrane tension (see Fig. 8 in Ref. [8]). Thus, while tension-induced changes appear not to affect the probability of defect formation in tether formation studies, in other situations in which membrane force resultants or electric fields are large, a dependence of pore formation probability on external forces could have a significant influence on membrane behavior.

These calculations are relevant for understanding the fundamental mechanisms underlying a wide variety of biological processes involving membrane asymmetry and membrane deformation. Incorporation of molecules preferentially into one leaflet of a bilayer has long been recognized to drive shape transformations in membranes [41,42]. However, when membrane shape is constrained by external forces or by associations with the cytoskeleton, preferential incorporation of molecules produces stress differences between the membrane leaflets [43]. If the membrane does not deform to relax these stresses, transport of molecules between leaflets will result. For example, enzymes involved in synthesis of phosphatidylcholine are confined to the cytoplasmic face of the endoplasmic reticulum. Preferential incorporation of molecules into one leaflet would result in rapid vesiculation of these structures, except that associations with cytoskeletal filaments constrain the geometry of the reticulum [44,45]. The resulting stress differences could drive interleaflet transport and account in part for the rapid flip-flop rates measured in these membranes [46]. Additionally, rapid interleaflet exchange has been observed during membrane fusion [47] that may have been promoted by the high curvature and interleaflet stress differences that occur during fusion. Interestingly, the time constants for the rapid exchange agreed with those measured in the tether experiments [8]. A similar mechanism may operate in red blood cell membrane because of the constraint on membrane shape caused by the membrane skeleton. Preferential transport of phosphatidylserine and phosphatidylethanolamine via the phospholipid translocase will generate stress differences between the membrane leaflets and drive a compensatory transport of lipid to the opposite leaflet. Indeed, such a mechanism appears to be required for the nonspecific transport of lipids needed to explain the maintenance of lipid asymmetry in red cell membrane [11,12,48].

ACKNOWLEDGMENTS

The authors are grateful to Dr. Ole Mouritsen, Dr. John Kolassa, Dr. Aleksander Popel, and Dr. Tilak Ratnanather for discussions. This work was supported by the US Public Health Service via the National Institute of Health Grant No. RO1-HL31524, and by the Ministry of Science and Technology of the Republic of Slovenia via the Grant No. 3411-99-71-0003.

[1] E. M. Bevers, P. Comfurius, D. W. C. Dekkers, and R. F. A. Zwaal, Biochim. Biophys. Acta **1439**, 317 (1999).
[2] R. F. A. Zwaal and A. J. Schroit, Blood **89**, 1121 (1997).
[3] E. Farge, D. M. Ojcius, A. Subtil, and A. Dautry-Varsat, Am. J. Physiol. **276**, C725 (1999).
[4] E. M. Bevers, P. Comfurius, D. W. C. Dekkers, M. Harmsma, and R. F. A. Zwaal, Biol. Chem. **379**, 973 (1998).
[5] K. Maiese and A. M. Vincent, J. Neurosci. Res. **59**, 568 (2000).
[6] J. E. Rothman and E. A. Dawidowicz, Biochemistry **14**, 2809 (1975).
[7] R. Homan and H. J. Pownall, Biochim. Biophys. Acta **938**, 155 (1988).
[8] R. M. Raphael and R. E. Waugh, Biophys. J. **71**, 1374 (1996).
[9] S. Svetina, B. Žekš, R. E. Waugh, and R. M. Raphael, Eur. Biophys. J. **27**, 197 (1998).
[10] D. V. Zhelev, Biophys. J. **71**, 257 (1996).
[11] S. Frickenhaus and R. Heinrich, Biophys. J. **76**, 1293 (1999).
[12] S. Frickenhaus and R. Heinrich, J. Theor. Biol. **197**, 175 (1999).
[13] P. F. Devaux, Biochemistry **30**, 1163 (1991).
[14] W. C. Wimley and T. E. Thompson, Biochemistry **30**, 1702 (1991).
[15] E. A. Evans and A. Yeung, Chem. Phys. Lipids **73**, 39 (1994).
[16] A. Yeung and E. Evans, J. Phys. II **5**, 1501 (1995).
[17] E. Evans, A. Yeung, R. Waugh, and J. Song, in *The Structure and Conformation of Amphiphilic Membranes*, Springer Proceedings in Physics, Vol. 66, edited by R. Lipowsky, D. Richter, and K. Kremer (Springer-Verlag, Berlin, 1992), p. 148.
[18] A. Yeung, Ph.D. thesis, Department of Physics, University of British Columbia, Canada, 1994.
[19] R. M. Raphael, Ph.D. thesis, Department of Biophysics, University of Rochester, Rochester, NY, 1996.
[20] R. N. Hall, J. Appl. Phys. **20**, 925 (1949).
[21] H. S. Carslaw and J. C. Jaeger, *Conduction of Heat in Solids* (Oxford University Press, London, 1959).
[22] R. E. Waugh, J. Song, S. Svetina, and B. Žekš, Biophys. J. **61**, 974 (1992).
[23] B. Božič, S. Svetina, B. Žekš, and R. E. Waugh, Biophys. J. **61**, 963 (1992).
[24] J. H. Ipsen, K. Jørgensen, and O. G. Mouritsen, Biophys. J. **58**, 1099 (1990).
[25] A. G. Lee, Biochemistry **16**, 835 (1977).
[26] D. Papahadjopoulous, K. Jacobson, S. Nir, and T. Isac, Biochim. Biophys. Acta **311**, 330 (1973).
[27] P. C. Noordam, A. Killian, R. F. M. O. Elferink, and J. de Gier, Chem. Phys. Lipids **31**, 191 (1982).
[28] S. W. Hui, Comments Mol. Cell. Biophys. **4**, 233 (1987).
[29] S. W. Hui and A. Sen, Proc. Natl. Acad. Sci. U.S.A. **86**, 5825 (1989).
[30] J. de Gier, Chem. Phys. Lipids **64**, 187 (1993).
[31] S. Paula, A. G. Volkov, A. N. Van Hoek, T. H. Haines, and D. W. Deamer, Biophys. J. **70**, 339 (1996).
[32] T. Honger, K. Jørgensen, D. Stokes, R. L. Biltonen, and O. G. Mouritsen, Methods Enzymol. **286**, 168 (1997).
[33] J. A. F. Op den Kamp, M. Th. Kauerz, and L. L. M. Van Deenen, Biochim. Biophys. Acta **406**, 169 (1975).
[34] A. Genz and J. F. Holzwarth, Eur. Biophys. J. **13**, 323 (1986).
[35] A. Genz, J. F. Holzwarth, and T. Y. Tsong, Biophys. J. **50**, 1043 (1986).
[36] D. V. Zhelev and D. Needham, Biochim. Biophys. Acta **1147**, 89 (1993).
[37] J. D. Moroz and P. Nelson, Biophys. J. **72**, 2211 (1997).
[38] J. C. Shillcock and D. H. Boal, Biophys. J. **71**, 317 (1996).
[39] W. Vaz, Z. Derzko, and K. Jacobson, *Membrane Reconstitution*, edited by G. Poste and G. L. Nicholson (Elsevier Biomedical, Amsterdam, 1982) pp. 83–136.
[40] J. D. Litster, Phys. Lett. **53A**, 193 (1975).
[41] M. P. Sheetz and S. J. Singer, Proc. Natl. Acad. Sci. U.S.A. **71**, 4457 (1974).
[42] S. Svetina and B. Žekš, Eur. Biophys. J. **17**, 101 (1989).
[43] R. E. Waugh, Biophys. J. **70**, 1027 (1996).
[44] S. L. Dabora and M. P. Sheetz, Cell **54**, 27 (1988).
[45] M. Terasaki and T. S. Reese, Cell Motil. Cytoskel. **29**, 291 (1994).
[46] W. R. Bishop and R. M. Bell, Annu. Rev. Cell Biol. **4**, 579 (1988).
[47] B. R. Lentz and J. K. Lee, Mol. Membr. Biol. **16**, 279 (1999).
[48] M. Brumen, R. Heinrich, A. Herrmann, and P. Müller, Eur. Biophys. J. **22**, 213 (1993).